

Solvent-induced current-voltage hysteresis and negative differential resistance in molecular junctions

Alan A. Dzhiyev* and D. S. Kosov

Department of Physics, Université Libre de Bruxelles, Campus Plaine, CP 231, Boulevard du Triomphe, BE-1050 Brussels, Belgium

(Received 13 January 2012; published 25 January 2012)

We consider a single molecule circuit embedded into solvent. The Born dielectric solvation model is combined with Keldysh nonequilibrium Green's functions to describe the electron-transport properties of the system. Depending on the dielectric constant, the solvent induces multiple nonequilibrium steady states with corresponding hysteresis in molecular current-voltage characteristics as well as negative differential resistance. We identify the physical range of solvent and molecular parameters where the effects are present. The position of the negative differential resistance peak can be controlled by the dielectric constant of the solvent.

DOI: [10.1103/PhysRevB.85.033408](https://doi.org/10.1103/PhysRevB.85.033408)

PACS number(s): 72.10.Bg, 05.60.Gg, 05.30.-d

The use of molecules—either singly or in small ensembles—as the elements of electronic circuits holds substantial promise in the fields of informational technology, biological and environmental nanosensors, and energy harvesting.¹ For the science of molecular electronics to be transformed into a technology it is not only important to fabricate stable molecular junctions but also to be able to efficiently control and manipulate their electric properties. In the silicon-based microelectronic technology the gate voltage regulates the flow of electrons, but placing a third gate electrode has proven to be difficult in single molecular size devices. The negative differential resistance (NDR) also plays an important role in semiconductor devices, because circuits with complicated functions can be implemented with significantly fewer components with its help. On the other hand, instead of copying the existing paradigms, such as, for example, gate voltage or resonant tunneling diode structure for NDR, the molecular electronics create new and unique opportunities. The “wet” molecular electronics, where solvent controls the electric behavior of an electronic circuit, may open a new chapter in device engineering. Indeed, some molecular electronic devices already exploit the solvent around the molecule to modulate conductance through alteration of the charge state or polarizability of the molecule.²⁻⁴

Let us consider a wet molecular circuit—a molecule attached to two macroscopic metal electrodes and embedded into solvent (Fig. 1). The total Hamiltonian is

$$H = H_L + H_R + H_M + H_T + H_{MS}. \quad (1)$$

The left and right electrodes contain free electrons and are described by the following Hamiltonians:

$$H_L = \sum_{l\sigma} \varepsilon_l a_{l\sigma}^\dagger a_{l\sigma}, \quad H_R = \sum_{r\sigma} \varepsilon_r a_{r\sigma}^\dagger a_{r\sigma}. \quad (2)$$

Here $a_{l\sigma}^\dagger$ creates an electron with spin σ in the single-particle state l/r of the left/right electrode and $a_{l\sigma}$ is the corresponding electron annihilation operator. The molecule is described by a single spin degenerate electronic level with energy ε_0 :

$$H_M = \varepsilon_0 \sum_{\sigma} a_{\sigma}^\dagger a_{\sigma}. \quad (3)$$

The operator $a_{\sigma}^\dagger(a_{\sigma})$ creates (destroys) an electron with spin σ on the molecular level. The tunneling coupling between the molecule and electrodes is

$$H_T = \sum_{l\sigma} t_l(a_{l\sigma}^\dagger a_{\sigma} + h.c.) + \sum_{r\sigma} t_r(a_{r\sigma}^\dagger a_{\sigma} + H.c.). \quad (4)$$

The interaction between the molecule and the surrounding solvent, H_{MS} , will be discussed below. We use natural units in equations throughout the paper: $\hbar = k_B = |e| = 1$, where $-|e|$ is the electron charge.

We describe the interaction between the molecule and the solvent based on the following simple model. The molecule is considered as a conducting sphere of radius R , and the solvent is macroscopically uniform and characterized by dielectric constant ϵ . The work needed to place charge q_M on a conducting sphere in the dielectric environment is given by the Born expression for the dielectric solvation energy:⁵

$$W = \frac{q_M q_S}{2R} \left(1 - \frac{1}{\epsilon}\right), \quad (5)$$

where q_S is the induced charge in the solvent ($q_M = -q_S$). The model can be easily extended to the molecules of complex shapes (the so-called generalized Born model, which represents the molecule as a number of overlapping spheres of different radii).⁶ The (generalized) Born model is quite simple yet is very successful in computing the electrostatic contribution to the solvation free energy.^{6,7} The solvent dynamics is slow in comparison with the electron tunneling time scale. For example, the dielectric relaxation of the solvent is diffusive and occurs on the picosecond or slower time scales since dipolar solvent molecules generally respond to the change of the molecule junction charging state by rotating.⁵ Therefore, we can assume that the induced charge q_S corresponds to the average electronic population of the molecular junction. Then, the dielectric solvation energy can be directly associated with the interaction of the molecule with the surrounding solvent:

$$H_{MS} = -U(\epsilon)(N - \delta)(\langle N \rangle - \delta), \quad (6)$$

where $U(\epsilon) = \frac{1}{2R}(1 - \frac{1}{\epsilon})$ is an effective, local, and solvent-controlled electron-electron attraction, and $N = \sum_{\sigma} a_{\sigma}^\dagger a_{\sigma}$. The charge of the molecule due to nonequilibrium tunneling of electrons is $(N - \delta)$, while $(\delta - \langle N \rangle)$ is the corresponding

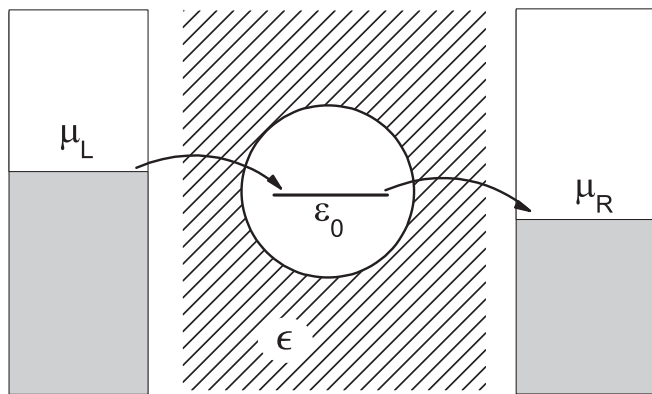


FIG. 1. Schematic illustration of the model. The molecule is attached to two metal electrodes and surrounded by solvent. The solvent is described by uniform dielectric constant ϵ .

induced charge in the solvent. The parameter δ is the equilibrium molecular electronic population, which depends on the position of the molecular level ϵ_0 relative to the electrode Fermi energy ϵ_f . If ϵ_0 corresponds to the highest occupied molecular orbital (i.e., $\epsilon_0 < \epsilon_f$), then, without the applied voltage bias, the molecular level is double occupied and $\delta = 2$. If ϵ_0 is the lowest unoccupied molecular orbital (i.e., $\epsilon_0 > \epsilon_f$), then the molecular level is empty in equilibrium and $\delta = 0$. It is known that such model Hamiltonians generally lead to bistable solutions.^{8,9} We emphasize that the model is not only applicable to the solvated molecular junction but also to the often employed experimental setting when the junction is embedded into isolating or semiconductor molecular film. In this case the surrounding molecular film can be considered as a macroscopic dielectric environment.

The similar mean-field-type interaction between the molecule and the solvent [Eq. (6)] can be also obtained within the polaron model in the limit $\omega/\Gamma \ll 1$ (here ω is the frequency of a characteristic vibrational mode coupled to the electrons and Γ is the broadening of the molecular level due to coupling to the metal electrodes).^{10,11} In our case ω is related to the dielectric relaxation of the solvent, which occurs on the picosecond and slower time scales, so $\omega \sim 0.001$ eV. For molecules interacting with the metal electrodes, $\Gamma \sim 0.1$ – 1 eV, which makes the static, effective mean-field (i.e., the static, average polarization of the solvent) approximation Eq. (6) exactly valid for our case.

Thus, in the Born approximation, the Hamiltonian $H_M + H_{MS}$ is exactly reduced to a spin degenerate single-level model with a local mean-field attractive interaction between electrons, which can be controlled by the dielectric constant of the environment. To describe electron transport through the system we use Keldysh nonequilibrium Green's-function formalism.^{12,13} The exact nonequilibrium molecular population $\langle N \rangle$ and electric current J become

$$\langle N \rangle = \frac{2}{\pi} \int d\omega \frac{\Gamma_L(\omega)f_L(\omega) + \Gamma_R(\omega)f_R(\omega)}{[\omega - \epsilon - 2\Lambda(\omega)]^2 + [\Gamma(\omega)]^2}, \quad (7)$$

$$J = \frac{4}{\pi} \int d\omega \frac{\Gamma_L(\omega)\Gamma_R(\omega)[f_L(\omega) - f_R(\omega)]}{[\omega - \epsilon - 2\Lambda(\omega)]^2 + [\Gamma(\omega)]^2}. \quad (8)$$

Here $f_{L/R}(\omega) = [1 + e^{(\omega - \mu_{L/R})/T}]^{-1}$ is the Fermi-Dirac distribution for electrons in the electrodes, $\epsilon = \epsilon_0 - U(\epsilon)(\langle N \rangle - \delta)$ is the effective energy of the molecular level, and $\Lambda = \Lambda_L + \Lambda_R$, $\Gamma = \Gamma_L + \Gamma_R$ are the real and imaginary parts of the electrode self-energy:

$$\Sigma_{L/R} = \sum_{k \in l/r} \frac{t_k^2}{\omega - \epsilon_k + i\eta} = \Lambda_{L/R}(\omega) - i\Gamma_{L/R}(\omega). \quad (9)$$

The electrodes are modeled as a semi-infinite chain of atoms, characterized by the voltage-dependent on-site energy $\mu_{L,R} = \pm V/2$ and the intersite hopping parameter $V_h = 2.5$ eV. The expression for the electrode self-energy can be found, for example, in Ref. 14. The electrode bandwidth $[\mu_{L/R} - 2V_h, \mu_{L/R} + 2V_h]$ is half filled, so the Fermi energy coincides with the on-site energy. The coupling between the left/right electrode edge and the molecule is taken to be $\sqrt{V_h\Gamma_0}$, where $\Gamma_0 = \Gamma_L(\mu_L) = \Gamma_R(\mu_R)$ is the maximal broadening of the molecular electronic level due to the coupling to the electrodes. Below we focus on the case when ϵ_0 is lower than the electrode equilibrium Fermi energy. All our results also remain qualitatively valid when ϵ_0 is above the Fermi level.

To compute the current, we first should determine the nonequilibrium molecular population (N). Since Eq. (7) is nonlinear, it generally has multiple solutions. Figure 2 shows the graphical solution of this equation. As we see, likewise for the electron transport in the polaron model,⁹ depending on the values of $U(\epsilon)$ and the molecular level energy ϵ_0 , Eq. (7) can have one, three, or even five solutions (the nonequilibrium fixed points). These multiple solutions may or may not be steady states (i.e., the stable fixed point). Following our method described in Ref. 15 we obtain the stability matrix and analyze the real part of its spectrum to assess the asymptotic time behavior of the fixed points. We find that only the two outer and the middle solutions are stable in the five-solution case (right panel in Fig. 2); i.e., they correspond to physically

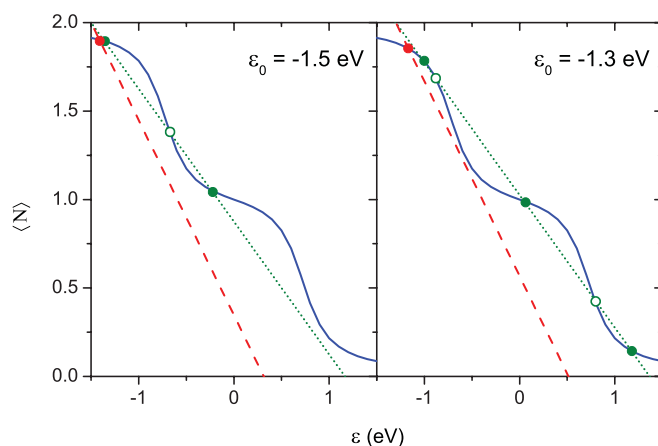


FIG. 2. (Color online) Graphical solution of Eq. (7). The straight lines are given by equation $\langle N \rangle = -\frac{\epsilon}{U(\epsilon)} + (2 + \frac{\epsilon_0}{U(\epsilon)})$. Depending on ϵ and ϵ_0 there can exist one, three, or five fixed-point nonequilibrium molecular populations. Filled circles represent stable steady-state populations, while open ones correspond to unstable fixed-point solutions of Eq. (7). Parameters: applied voltage bias $V = 1.5$ eV, $T = 300$ K, $\Gamma_0 = 0.1$ eV, $R = 10$ bohrs, $\epsilon = 50$ (dotted lines), and $\epsilon = 3$ (dashed lines).

realizable nonequilibrium steady-state populations. In the case of three solutions (left panel in Fig. 2), the middle solution is unstable and the other two fixed points are stable. We note that our approach is immune from the criticism that the observed multiple steady states are artifacts of the mean-field and electron self-interaction.¹⁶ The effect of self-interaction is physically present in our case, since an electron in the molecule interacts with its own induced charge in the solvent.

Let us now establish the range of key physical parameters—dielectric constant ϵ , molecular size R , and molecular level energy ϵ_0 , which allow the existence of multiple nonequilibrium steady states. For presentation purposes we assume that the molecular level broadening, Γ_0 , as well as the temperature are much smaller than applied voltage V . Therefore the molecular population [Eq. (7)] (solid lines in Fig. 2) can be approximated by a steplike function of energy ϵ . Then, we can readily determine analytically the conditions on ϵ_0 and $U(\epsilon)$ when Eq. (7) has only one solution. In Fig. 3 we show the domain where multiple steady states exist for the case $\epsilon_0 < 0$. The case $\epsilon_0 > 0$ can be considered in the same way, and the resulting multistability domain is a mirror reflection of that in Fig. 3 across the abscissa axis.

In Fig. 4, we show the behavior of the level population and the current as a function of applied voltage. Due to the presence of multiple steady states, both the population and the electron current demonstrate a hysteresis behavior. The width of the hysteresis loop is proportional to $U(\epsilon)$ and, therefore, it can be controlled by the dielectric constant. It should be emphasized that the solvent-induced hysteresis loop can be observed at moderate applied voltages where the molecular device is still mechanically stable. Moreover, the nonlinearity in the molecule-solvent interaction leads to NDR features in the current-voltage characteristic (the drop in the current represented by the dashed line at around 1 eV of applied voltage in Fig. 4). The NDR appears when one of the electrode chemical potentials crosses the position of the molecular level. Then, due to the subsequent shift in the level energy caused by

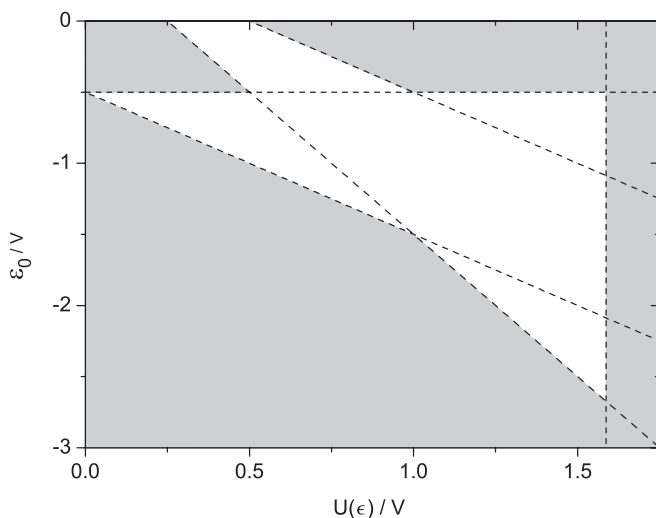


FIG. 3. (White domain) Values of ϵ_0 and $U(\epsilon)$ where the multiple steady-state solutions exist ($\Gamma_0/V \ll 1$). Dashed lines determine the domain boundary, and they are $\epsilon_0 = -0.5V$, $\epsilon_0 = -U + 0.5V$, $\epsilon_0 = -U - 0.5V$, $\epsilon_0 = -2U + 0.5V$, and $U = 1/2R$.

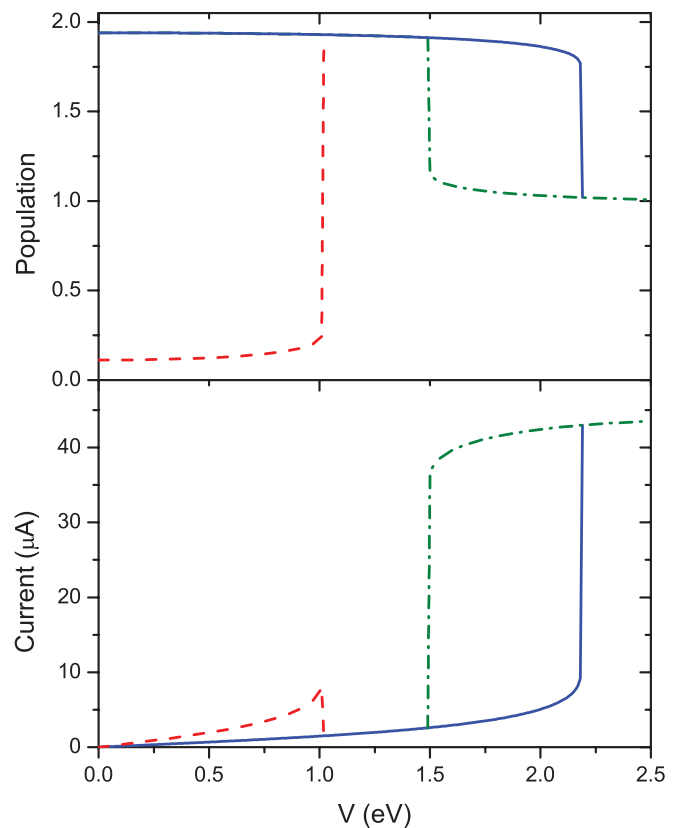


FIG. 4. (Color online) Population-voltage and current-voltage characteristics. Parameters are $T = 300$ K, $\epsilon_0 = -1.6$ eV, $R = 10$ bohrs, $\epsilon = 50$, and $\Gamma_0 = 0.1$ eV. Three curves correspond to three possible roots of Eq. (7): solid line, upper root; dashed line, lower root; and dash-dotted line, middle root.

the electronic population change, the level moves away from the current-carrying window between the chemical potentials. In the case of $\epsilon_0 < -0.5U(\epsilon)$, shown in Fig. 4, the NDR takes place when we begin with the empty level. When ϵ_0 lays above $-0.5U(\epsilon)$ ($\epsilon_0 < 0$) the NDR also takes place, but in this case we need to start from the initially fully occupied level.

The NDR in the wet molecular circuit turns out to be sensitive to the dielectric constant of the environment. Figure 5 shows the dependence of the NDR peak position on the dielectric constant of the solvent. The increase of the solvent polarity shifts the peak toward the higher voltages. This effect is very robust. It does not require an artificial tuning of the model parameters and holds at very large ranges of temperatures. The temperature dependence of the NDR peak (inset in Fig. 5) is consistent with experimental observations,^{17,18} and in contrast to the polaron model explanation of NDR⁹ does not require unphysical values for the parameters.

We would like to comment here on the importance of the time scales. Depending on the relative time scales of measurements and transitions between stable fixed points, the multistability can result in merely noise associated with the jumps between steady states or it can lead to hysteresis and NDR.¹⁹ To be experimentally resolved the transition rate between multiple steady states should be smaller than the typical observation time. In our case

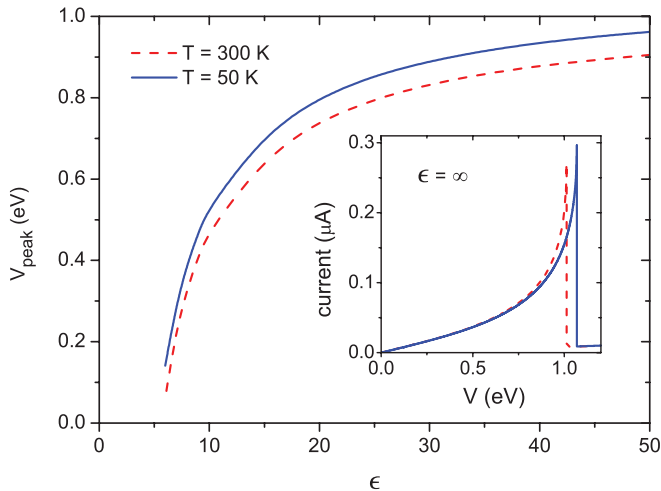


FIG. 5. (Color online) NDR peak voltage value as a function of the dielectric constant for two different temperatures. Parameters are $\epsilon_0 = -2.0$ eV, $R = 10$ bohrs, and $\Gamma_0 = 0.01$ eV. Inset: NDR in the current-voltage characteristic for $\epsilon = \infty$.

the transition between steady states is determined by the very slow diffusive reorganization of the solvent, which opens a possibility for experimental realization of the proposed effects.

In conclusion, we have presented a theoretical model to describe the environmental control of the electron-transport

properties of wet molecular junctions. The interaction between the molecule and solvent leads to effective attraction between electrons which is governed by the dielectric constant of the surrounding solvent. The natural separation of electronic and solvent time scales makes the mean-field consideration exact for our model. We used Keldysh nonequilibrium Green's functions to obtain a nonlinear equation for molecular population and electric current. Depending on the dielectric constant, the inherent nonlinearity of molecule-solvent interactions induces multiple nonequilibrium steady states with corresponding hysteresis in molecular I-V characteristics as well as NDR. We identify the physical range of solvent and molecular parameters which allows the appearance of multiple steady states. The temperature effects on the NDR peak are in qualitative agreement with the available experimental data. We demonstrated that the dielectric constant of the solvent can be used as a control parameter which regulates the position of the NDR peak.

ACKNOWLEDGMENTS

This work has been supported by the Francqui Foundation, Belgian Federal Government, under the Inter-University Attraction Pole project NOSY, and Programme d'Actions de Recherche Concertée de la Communauté Française (Belgium), under project "Theoretical and experimental approaches to surface reactions."

*On leave of absence from Bogoliubov Laboratory of Theoretical Physics, Joint Institute for Nuclear Research, RU-141980 Dubna, Russia.

¹M. Galperin, M. A. Ratner, A. Nitzan, and A. Troisi, *Science* **319**, 1056 (2008).

²X. Y. Xiao, L. A. Nagahara, A. M. Rawlett, and N. J. Tao, *J. Am. Chem. Soc.* **127**, 9235 (2005).

³F. Chen, J. He, C. Nuckolls, T. Roberts, J. Klare, and S. Lindsay, *Nano Lett.* **5**, 503 (2005).

⁴G. Morales, P. Jiang, S. Yuan, Y. Lee, A. Sanchez, W. You, and L. Yu, *J. Am. Chem. Soc.* **127**, 10456 (2005).

⁵A. Nitzan, *Chemical Dynamics in Condensed Phases* (Oxford University Press, Oxford, 2006).

⁶D. Bashford and D. A. Case, *Annu. Rev. Phys. Chem.* **51**, 129 (2000).

⁷A. R. Leach, *Molecular Modeling. Principles and Applications* (Pearson, Harlow, 2001).

⁸A. S. Alexandrov, A. M. Bratkovsky, and R. S. Williams, *Phys. Rev. B* **67**, 075301 (2003).

⁹M. Galperin, M. A. Ratner, and A. Nitzan, *Nano Lett.* **5**, 125 (2005).

¹⁰A. M. Kuznetsov, *J. Chem. Phys.* **127**, 084710 (2007).

¹¹M. Galperin, A. Nitzan, and M. A. Ratner, *J. Phys. Condens. Matter* **20**, 374107 (2008).

¹²L. V. Keldysh, *Zh. Eksp. Teor. Fiz.* **47**, 1515 (1965) [*Sov. Phys. JETP* **20**, 1018 (1965)].

¹³H. Haug and A. Jauho, *Quantum Kinetics in Transport and Optics of Semiconductors* (Springer, Berlin, 2010).

¹⁴U. Peskin, *J. Phys. B* **43**, 153001 (2010).

¹⁵A. A. Dzhioev and D. S. Kosov, *J. Chem. Phys.* **135**, 174111 (2011).

¹⁶A. S. Alexandrov and A. M. Bratkovsky, e-print arXiv:cond-mat/0603467v3.

¹⁷J. Chen, M. A. Reed, A. M. Rawlett, and J. M. Tour, *Science* **286**, 1550 (1999).

¹⁸J. Chen and M. A. Reed, *Chem. Phys.* **281**, 127 (2002).

¹⁹E. Lörtscher, J. W. Ciszek, J. Tour, and H. Riel, *Small* **2**, 973 (2006).